Millimeter-Wave Propagation Characteristics Analysis for Vehicle to Infrastructure Communication

Yaser Bakhuraisa
Faculty of Engineering and Technology
Multimedia University
Melaka, Malaysia
1211400159@student.mmu.edu.my

Azlan Bin Abd Aziz
Faculty of Engineering and Technology
Multimedia University
Melaka, Malaysia
azlan.abdaziz@mmu.edu.my

Tan Kim Geok
Faculty of Engineering and Technology
Multimedia University
Melaka, Malaysia
kgtan@mmu.edu.my

Saifulnizan Jamian
Faculty of Mechanical and Manufacturing Engineering
Universiti Tun Hussein Onn Malaysia
Selangor, Malaysia
saifulnz@uthm.edu.my

Mohamad Yusoff Alias
Faculty of Engineering
Multimedia University
Selangor, Malaysia
yusoff@mmu.edu.my

Mohd Khanapiah Bin Nor
Faculty of Technology and Engineering
Universiti Teknikal Malaysia Melaka
Melaka, Malaysia
khanapiah@utem.edu.my

2024 IEEE 7th International Symposium on Telecommunication Technologies (ISTT) | 979-8-3503-9207-4/24/$31.00 ©2024 IEEE | DOI: 10.1109/ISTT63363.2024.10750611

***Abstract*—Waveform-based localization approaches are considered the most reliable for vehicles in complex heterogeneous environments. However, this paper addresses millimeter-wave (mm-wave) propagation for vehicle to infrastructure (V2I) scenario at 28 GHz and 73 GHz. Particularly, it analyses the key localization elements for waveform-based approach such as received power and angel of arrival. Additionally, this paper investigates the impact of vehicles mobility on the stability these key elements at a certain position. Ray tracing techniques have been used to model the propagation characteristics of the aforementioned bands of mm-wave at a semirealistic V2I communication scenario. The obtained results indicated a proportional correlation between the received power and the elevation angle of arrival at a given location, potentially enhancing localization performance. In the other side, the mobility speed of the vehicle showed a notable impact on the stability of the key localization elements at a certain location.**

Keywords—V2I, mm-wave, ray tracing, power angle profile, vehicle mobility.

I. INTRODUCTION

Millimeter-wave (mm-wave) provides a high bandwidth. Therefore, it has been involved in the current vehicles communications to meet the growing demand for large data transmission. This has inspired numerous researchers to leverage its propagation properties for vehicle localization, aiming to address the limitations of GPS in challenging environments such as urban areas [1]. However, localization techniques of mm-wave can be categorized into two main approaches: message-based approach and waveform-based approach [2]. The authors in [3] mentioned that, the waveform-based approaches are the most promising in the complex environments due to the higher estimation accuracy of its propagation features thanks to enabling narrow beam and Multiple-Input Multiple-Output (MIMO) technology. However, in order to provide a high positioning accuracy based on waveform-based approaches, it is important to analyze the characteristics of the mm-wave. However, the analysis of path propagation characteristics of mm-wave communication had been proposed in the literature with different frequencies [4][5][6][7]. To the best of the authors' knowledge, the majority of previous studies have focused on evaluating network performance; meanwhile the analysis regarding the localization purposes is still limited.

In the analysis for localization purposes, the so called key localization elements such as received power (also called received signal strength (RSS)), propagation delay time, and angular characteristics including angle of arrival (AOA) and angle of departure (AOD) should be considered [8]. These key localization elements play a vital role in waveform-based localization approaches, whether they are geometric-based [9] or fingerprinting-based [10].

The characteristics of mm-wave are greatly affected by the type of the propagation path. Due to the short wavelength, mm-wave propagation paths can be strongly affected by small obstacles scattering objects [11]. Therefore, the propagation of multipath of mm-wave in urban environments is a complex phenomenon. However, modeling the propagation characteristics of mm-wave bands is a crucial step in the analysis process. Different methods have been utilized to model the mm-wave propagation paths. It can be classified to stochastic and deterministic models [12]. In stochastic models, the channel measurement validation still critical due to the large assumptions. The deterministic models, in contrast, are more accurate for modeling the propagation characteristics of mm-wave. It had been widely utilized to model the mm-wave in outdoor scenarios [13][14]. Ray tracing techniques are a deterministic model. It has a simi-reality performance to model the multipath propagation of mm-wave spatially when the detailed 3D environment is created [15]. Furthermore, the different propagation mechanisms, such as diffraction from sharp edges, reflections from smooth surfaces, transmission through different mediums, and scattering from rough surfaces or small objects, can be involved [16][17]. Therefore, it will be considered to model the propagation characteristics of mm-wave in this research.

In summary, this research aims to provide a comprehensive analysis of the mm-wave propagation characteristics at 28 GHz and 73 GHz in terms of received power and angular. However, in this work, the ray tracing technique based on Wireless Insite (WI) software is used to model vehicle-to-infrastructure (V2I) in urban environment to acquire the data of the mm-wave propagation paths. Kuala Lumpur City Centre (KLCC), Ampang Street is selected to be our study environment. 3D model of selected area of study is shown in Fig. 1. KLCC is selected as an example of a representative urban area for V2I communication analysis due to its highly dense urban environment, which poses unique

Fig.1. The reconstructed 3D of Ampang Street, KLCC

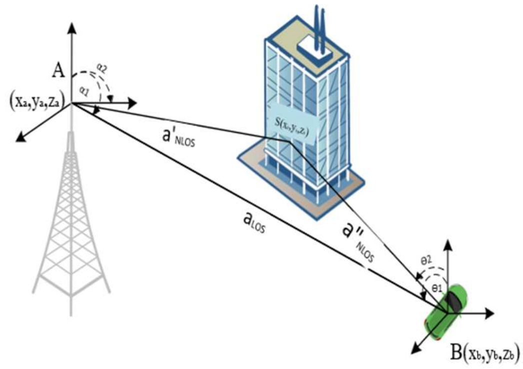

Fig.2. Elevation angles for LOS and NLOS scenarios

challenges for mm-wave propagation. The area is characterized by numerous tall buildings, which create a complex environment for signal transmission, with a high potential for signal reflections and scattering.

The structure of this article is organized as follows. Analysis of the key localization elements is presented in Section II. The fluctuation of the mm-wave characteristics over the mobility of the vehicle is investigated in Section III. Section IV presents the simulation setup and modeling of V2I communication scenario. Analysis of the simulation results is elaborated in section V. Finally, the conclusion is drawn in Section VI.

II. Analysis Of Key Localization Elements

This section presents an analysis of the key localization elements including received power, propagation delay time, and angular characteristics. Basically, the received power is function of the propagation path length [18]. In [19], the authors presented an analysis of received power for several mm-wave bands. Furthermore, they introduced analysis of propagation delay time. The findings of this analysis are the value of path loss is directly proportional to the frequency. However, according to the investigation results in [6] and [20], the authors conclude that the propagation delay doesn't affect by the frequency variation in LOS scenario. Whereas, in NLOS scenario, the delay spread is increase with decrease in frequency. However, the angle of arrival is usually utilized jointly with the previous parameters, i.e., RSS and delay of propagation, to improve the localization performance [21]. The angular characteristics have been analyzed earlier in [22] to distinguish the NLOS paths. In [23], a geometric relationship between the separated distance from the BS to the receivers and the elevation angle of arrival (EAOA) is analyzed to improve the accuracy of the proposed localization approach. However, according to the Theorem 1 in [22], the relationship between the EAOA of the received signal and the length of the established propagation path between the base station (BS) to the receivers can be described as follows

$$\tan\theta_1 = \frac{z(a) - z(b)}{\sqrt{(x(a)-x(b))^2+(y(a)-y(b))^2}} \quad (1)$$

$$\tan\theta_2 = \frac{z(s)-z(b)}{\sqrt{(x(s)-x(b))^2+(y(s)-y(b))^2}} \quad (2)$$

where θ is the EAOA, θ_1 for LOS scenario and θ_2 for NLOS scenario, as depicts in Fig. 2. From (1) and (2) above, it can be concluded that shorter propagation paths result in a smaller denominator and a reduced EAOA. In other words, when the EAOA of the received signal is larger, it is more likely that the propagation path between the base station and the vehicle is NLOS.

III. Analysis of Impact of Vehicle mobility on the mm-Wave Characteristics

As mentioned earlier, the fluctuation of the mm-wave characteristics, such as RSS and AOA, is considered the main challenge affecting the reliability of waveform-based localization systems. Indeed, in the context of wireless communication channels, the RSS components are distance and phase dependent, while, the angular components are spatial dependent. However, this section presents analysis of vehicle speed effect on the fluctuation of these characteristics at specific location. The aim of this analysis is to investigate how vehicle speed impacts these characteristics and to determine which of them are more stable against changes in vehicle speed.

Assuming that, for a given mm-wave V2I communication scenario, the vehicle travels several times (several trips) along a specific trajectory. The vehicle's velocity remains constat during the trip, but each trip has a different velocity. Therefore, the vehicle will move through each a specific location on the trajectory at varying speeds. In other words, the relative velocity between the transmitter and the vehicle varies at each specific location along the trajectory. Fig. 3 shows the concept of phase difference that experience the incident signal at the same antenna element due to change the relative speed between the transmitter and receiver at specific location.

However, the channel frequency response (CFR) for L received multipath components (MPCs) at a specific location can be expressed as follows [24]

$$H(f) = \sum_{\ell=1}^{L} \rho_\ell e^{-j(2\pi f_c \tau_\ell + \beta_\ell)} \cdot c(\Omega_\ell) \quad (3)$$

where, ρ_l is the complex amplitude or power of the l-th MPC (it depends on length of l-th MPC and multipath effect), f_c is carrier frequency, τ_l is time delay, $c(\Omega_l)$ is the AOA which describes the vertical and horizontal angle of incident, $\Omega_l = [\cos\emptyset_l \sin\theta_l, \sin\emptyset_l \sin\theta_l, \cos\theta_l]$, where $\emptyset_l$ and θ_l are, respectively, the horizontal and vertical AOA associated with the l-th MPC, and β_l is the phase component of the l-th MPC. The expression in (3) consists of two components. The first component is $(\rho_l\, e^{-j2\pi\beta_l\tau_l})$. It called temporal components

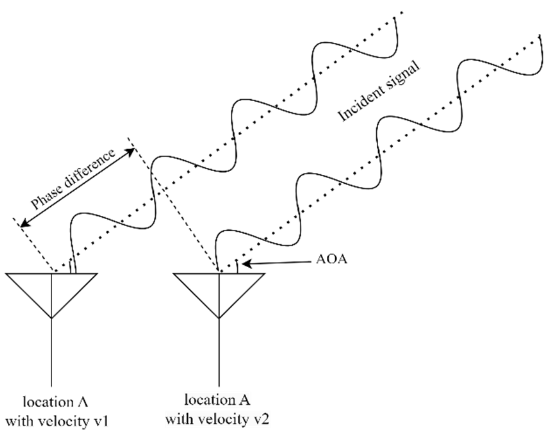

Fig.3. Phase difference of the incident signal at same antenna

(also known as RSS), it describes how the power of signal is changed in delay time and phase difference. Meanwhile the second component, $c(\Omega_l)$ is angular components, it also called spatial characteristics. However, we present analysis of the impact of vehicle speed on these components separately. In our scenario, the CIR is measured at a specific location on the trajectory. With the assumption that, at a specific location of V2I scenario, most of the propagated MPCs arrive at the receiver after they are reflected from fixed obstacles (buildings); therefore, the length of these MPCs can be considered constant. Note that, this assumption is reasonable where the structure of the V2I communication have special properties compared with V2V paths, such as the height of transmitter's antenna. Based on this consideration, the impact of path loss and multipath effect on the RSS fluctuation can be assumed to be constant, and the phase component, β_l solely has impact on characteristic's fluctuation. According to [2], the β_l can be expressed as follows

$$\beta_l = \frac{v\, f_c}{c}\cos(\alpha) \tag{4}$$

where, v is the vehicle speed, c is the speed of the light, and α is the angle between the arrived MPC and the vehicle motion direction. In our scenario concern with since we measure the CIR at specific location; therefore, the α is constant. However, from (4), it is clear that there is a linear dependency of change in the frequency β_l with the vehicle speed. In other words, with higher frequencies, such as mm-wave bands, a slight variation in relative speed leads noticeable change in β_l, and accordingly, the measured RSS at a specific location may fluctuate significantly.

However, given a uniform linear array (ULA), the AOA can be estimated using method commonly known as the Two-Step TDOA-AOA technique. This method combines time difference of arrival (TDOA) measurements between pairs of any two consecutive antenna elements with their geometry to estimate the angle of incident signal. The AOA can be calculated in this technique as follows

$$\Omega = sin\ (t_{ij}c/d_{ij}) \tag{5}$$

where t_{ij} is TDOA between antenna i and j elements, and d_{ij} is the distance between these antenna elements. The expression (5) shows that the AOA estimation relies on both TDOA and the geometry of the array antenna, making it less affected by changes in vehicle speed. This because these are not affected by the phase directly.

In summary, it can be inferred that at a specific location, the RSS may exhibit more noticeable variations compared to the AOA when there is a change in the relative speed between the vehicle and the RSU.

IV. Simulation Setup and V2I Configuration

In this section, the considered mm-wave V2I communication scenario is described. We adopted the geometry-based deterministic channel model for modeling the reflectors and V2I channel characterization. Particularly, ray tracing simulator, namely Wireless InSite (WI) software, is used for this task. It is worth mentioning that ray tracing methods have shown significant capability for predicting mm-wave channel propagation characteristics [3][16][17]. However, in order to construct a realistic V2I communication scenario, first a 3D city layout of Kuala Lumpur City Centre (KLCC), Ampang Street is created according to the detailed information in the reference [25]. Next, the 3D model is imported to WI as shown in Fig. 2. The material properties of buildings, terrain, vegetation, and objects (roads and vehicles) are defined based on the recommendations of the International Telecommunication Union (ITU) for a typical 5G mm-wave frequencies [26][27]. The material properties of the created environment and the V2I specifications are listed in Table 1. After that, we followed the reference [28] configurations to construct a V2I communication scenario. The transmitter (base station) is placed beside the street at (x=295m, y= 312m); whereas, several trajectories (receivers) are distributed to match the street lanes. The specifications of the constructed V2I are inspired by [29][30]. The operating frequency is 28GHz, and the antennas of transmitter and receiver half-wave dipole. However, following the mm-wave propagation mechanism, the transmission and diffraction are adjusted to zero, while the maximum number of reflections is

TABLE I. Parameters of Simulation Setup and V2I Configuration

EM of Material Properties			
Features Type	***Material***	ε_r	***σ[S/m]***
Buildings	Concrete	5.31	0.8967
Terrain	Medium dry ground	5.7	6.5
Vegetation	Foliage	26	0.39
Road	Asphalt	5.72	5e-4
Vehicle	Metal	4.00	1.5e-2
V2I Communication Settings			
Antenna Type		Half-wave dipole	
Antenna Polarization		Vertical	
Antenna Gain		27 dBi	
Antenna Height		BS = 10 m Vehicle = 2 m	
Transmitted power		32.0 dBm	
Operating Frequency		28 GHz	
Propagation model		X3D	

set to two [31]; moreover, diffuse scattering mode is enabled. Our scenario here is based on method known as beam-selection in V2I; therefore, for the given scenario, we set the vehicle to select the strongest five resolved links (paths).

However, through the considered propagation model of the ray tracing, the CIR of (1) is recorded at each location of the trajectories. However, based on simulation setup, and form a given reflector location, the CIR of each resolved path can be created. Accordingly, the corresponding propagation characteristics (RSS, EAOA, and AAOA) will be determined.

V. Results and Discussions

A. *Received Power Analysis*

In this section, the relationship between the received power and propagation delay. Fig. 4 displays the measured at the constructed trajectory for two frequency bands: 28 GHz (blue points) and 73 GHz (red points). The resolution of measurement was 1 m. Overall, both datasets show a clear trend where the RSS decreases as the distance from the transmitter increases, which is expected due to free-space path loss and other propagation effects. Moreover, the received power at 73 GHz is consistently lower than at 28 GHz, in accordance with the power law, which states that higher frequencies experience greater attenuation. From a localization standpoint, the figure highlights the challenges and opportunities in using RSS-based localization for mmWave communication systems. The scatter in the data points reveals variability in the measured RSS at specific distances.

B. *Power Angle Profile Analysis*

In this section, the analysis of distribution of azimuth angle of arrival (AAOA) and EAOA is presented; furthermore, we offer analysis of correlation the received power and EAOA. However, since we have observed that there are no significant variances of 28 GHz and 73 GHz, the analysis of angular profile in this section will only be confined to the simulation result of 28 GHz.

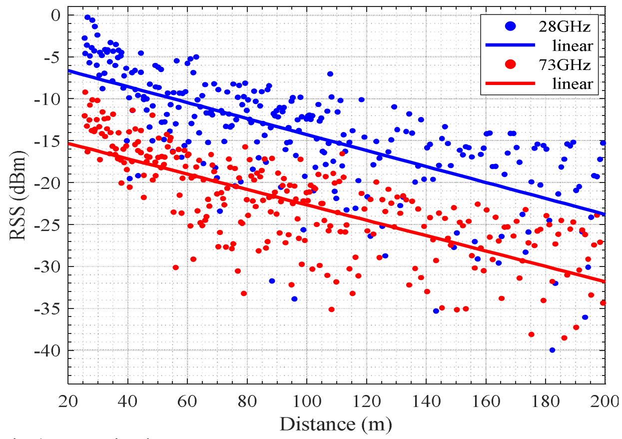

Fig.4. Received Power

For power angle profile (PAP) analysis, four receivers were chosen to represent the variation of PAP in both LOS (RX3 and RX4) and NLOS (RX1 and RX2) scenarios. As illustrated in Fig. 5, the received power in the LOS scenario exceeded that of the NLOS scenario, with maximum values of -13.20 dBm and -4.42 dBm for LOS, compared to -25.2573 dBm and -28.5965 dBm for NLOS. This confirms that the received power threshold effectively distinguishes between direct and reflected paths. Notably, the distribution of AAOA fluctuates in both scenarios, which is likely due to the arrangement of surrounding buildings.

Fig. 5 also presents the simulation results for the Elevation Angle of Arrival (EAOA) across the four receivers (in the right side). A clear difference in the distribution of received power with respect to EAOA between LOS and NLOS conditions is observed. The LOS scenario shows a broader range of EAOA distribution compared to the more concentrated range in the NLOS case. In the NLOS scenario, the majority of received signals are concentrated around 90°, indicating that most signals arrive almost horizontally after traversing long propagation paths. In contrast, for the LOS

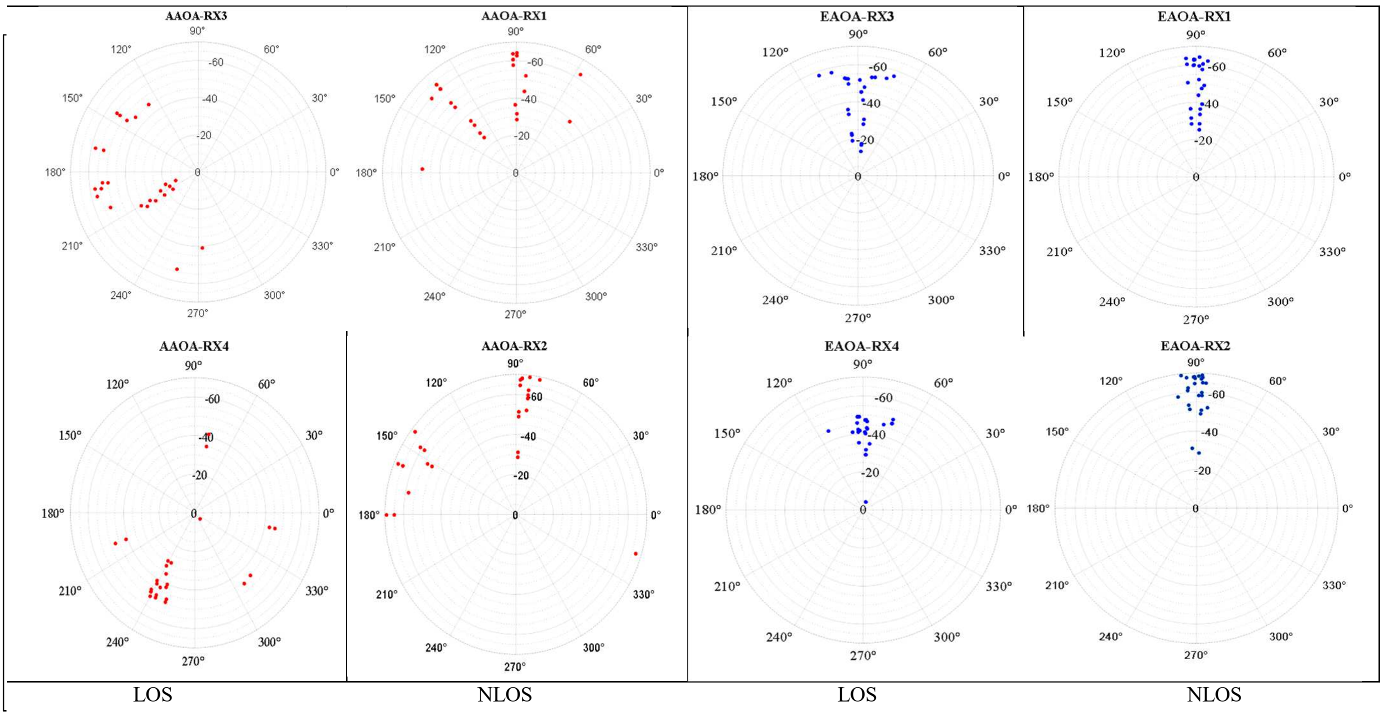

Fig.5. Power Angle Profile

receivers, the received power diminishes as the EAOA approaches 90°, with the strongest signals arriving from paths with the smallest EAOA.

C. Impact of Vehicle Mobility on Propagation Characteristics

To investigate the perturbation of the received power and angular characteristics of mm-wave signal due to the speed variation, we have recorded these characteristics along a constructed trajectories with vehicle speeds ranging from 10 km/h to 80 km/h. Fig. 6 illustrates the fluctuation in RSS of the mm-wave signal at four specific locations over the vehicle speed. Overall, the figure illustrates non-linear relationship between vehicle speed and RSS in mm-wave V2I communication scenarios suggests that the impact of vehicle speed on RSS is complex. The figure also demonstrates that the recorded RSS exhibits frequent fluctuations over a considerable range, highlighting the importance of robust localization systems capable of adapting to varying signal conditions.

However, upon investigating the channel propagation characteristics of mm-wave, we have found that the angular characteristics (i.e., EAOA and AAOA) show less influence by the speed of the vehicle. Fig. 7 illustrates the cumulative distribution function (CDF) of the standard deviations of mm-wave propagation characteristics for the constructed trajectories. It is clear that the special characteristics, i.e., AAOA and EAOA, exhibit greater stability compared to the RSS. Approximately more than 90% of the standard deviation of normalized EAOA and AAOA is nearly zero, i.e., there very low fluctuations in angular characteristics caused by the speed variation. Conversely, 90% of the values of RSS standard deviation are above 0.6. This lends support to the notion that deriving features from angular characteristics may enhance the reliability of the localization systems.

VI. CONCLUSION

This work aims to provide analysis of propagation characteristics, which are the key localization elements of waveform-based localization approach, of mm-wave for V2I communication scenario. The ray tracing technique is employed to model the propagation characteristics at 28 GHz and 73 GHz. The resulting propagation path characteristics are analyzed with respect to received power, propagation delay and angular characteristics. Based on this analysis we conclude that there is a proportional relationship between the

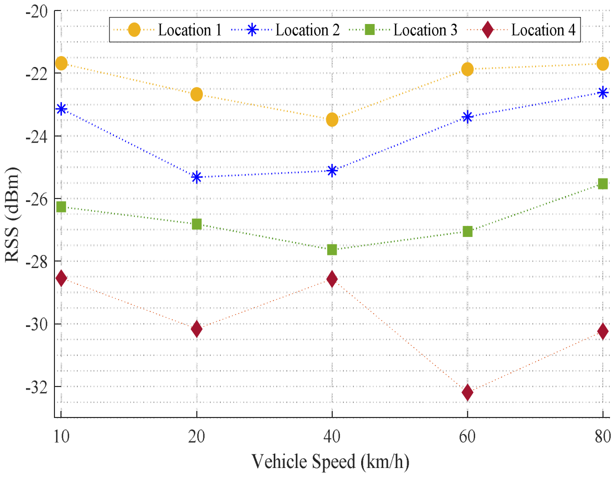

Fig.6. RSS variations at 4 samples

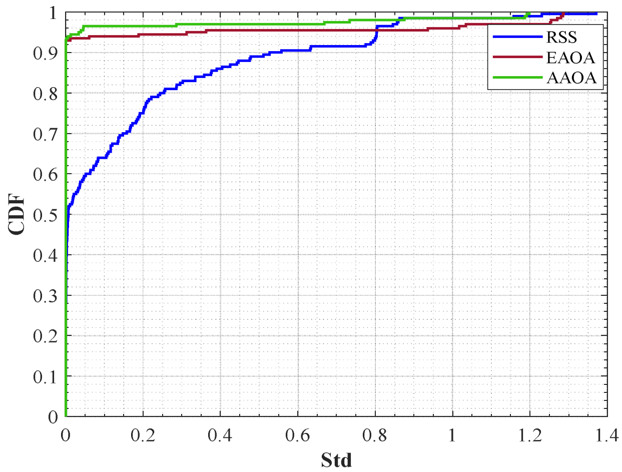

Fig.7. Standard deviations of mm-wave propagation characteristics

received power and the elevation angle of arrival at each specific location. In addition, such parameters play a significant part to understand the behavior of multipaths propagation in a complex environment to utilize them to improve the localization performance. We further investigated the impact of the vehicle mobility on the fluctuation of the propagation characteristics at a certain location. The investigation results showed a notable impact on the propagation characteristics. In future works the fluctuation of the propagation characteristics are suggested to study in terms of weather conditions and non-stationary obstacles.

ACKNOWLEDGMENT

This work was supported by the Ministry of Higher Education, Malaysia FRGS/1/2019/TK08/MMU/03/1.

REFERENCES

[1] S. Kuutti, S. Fallah, K. Katsaros, M. Dianati, F. Mccullough, and A. Mouzakitis, “A Survey of the State-of-the-Art Localization Techniques and Their Potentials for Autonomous Vehicle Applications,” *IEEE INTERNET THINGS J.*, vol. 5, no. 2, pp. 829–846, 2018.

[2] K. A. A. Mallak, M. Nair, G. Hilton, T. H. Loh, and M. A. Beach, “Characterising the Impact of Antenna Beamwidth on the Performance of Vehicle-to-Infrastructure (V2I) Millimetre Wave Communication,” in *2021 International Symposium on Networks, Computers and Communications, ISNCC 2021*, 2021, pp. 1–6. doi: 10.1109/ISNCC52172.2021.9615843.

[3] B. Neekzad, K. Sayrafian-pour, J. Perez, and J. S. Baras, “Comparison of Ray Tracing Simulations and Millimeter Wave Channel Sounding Measurements,” in *2007 IEEE 18th International Symposium on Personal, Indoor and Mobile Radio Communications*, 2007, pp. 1–5. doi: 10.1109/PIMRC.2007.4394537.

[4] M. Mahbub, M. M. Saym, and M. A. Rouf, “MmWave Propagation Characteristics Analysis for UMa and UMi Wireless Communications,” *2020 2nd Int. Conf. Sustain. Technol. Ind. 4.0, STI 2020*, vol. 0, pp. 19–20, 2020, doi: 10.1109/STI50764.2020.9350499.

[5] F. Fuschini, H. El-Sallabi, V. Degli-Esposti, L. Vuokko, D. Guiducci, and P. Vainikainen, “Analysis of Multipath Propagation in Urban Environment Through Multidimensional Measurements and Advanced Ray Tracing Simulation,” *IEEE Trans. Antennas Propag.*, vol. 56, no. 3, pp. 848–857, 2008, doi: 10.1109/TAP.2008.916893.

[6] V. Raghavan, A. Partyka, L. Akhoondzadehasl, A. Tassoudji, O. Koymen, and J. Sanelli, “Millimeter Wave Channel Measurements and Implications for PHY Layer Design,” *IEEE Trans. Antennas Propag.*, vol. 65, no. 12, pp. 6521–6533, 2017.

[7] X. Bian, Y. Liu, and S. Li, “Analysis of Millimeter-Wave Channel Characteristics in Urban Microcell Environment Based on the SBR Method,” in *2020 International Conference on Microwave and Millimeter Wave Technology, ICMMT 2020 - Proceedings*, 2020, pp. 7–9. doi: 10.1109/ICMMT49418.2020.9386788.

[8] Y. Bakhuraisa, A. A. Aziz, T. K. Geok, S. Jamian, and F. Mustakim, "A Survey of Ranging Techniques for Vehicle Localization in Intelligence Transportation System : Challenges and Opportunities," *Int. J. Electr. Comput. Eng.*, vol. 12, no. 6, pp. 6248–6260, 2022, doi: 10.11591/ijece.v12i6.pp6248-6260.

[9] K. Han, S. Ko, K. Huang, and S. Member, "Hidden Vehicle Sensing via Asynchronous V2V Transmission : A Multi-Path- Geometry Approach," *IEEE Access*, vol. 7, pp. 169399–169416, 2019, doi: 10.1109/ACCESS.2019.2954858.

[10] X. Gong, X. Yu, X. Liu, and X. Gao, "Machine Learning-Based Fingerprint Positioning for Massive MIMO Systems," *IEEE Access*, vol. 10, no. July, pp. 89320–89330, 2022, doi: 10.1109/ACCESS.2022.3199728.

[11] A. Al-saman *et al.*, "Survey of Millimeter-Wave Propagation Measurements and Models in Indoor Environments," *Electronics*, vol. 10, no. 1653, pp. 1–28, 2021.

[12] D. He, B. Ai, K. Guan, L. Wang, Z. Zhong, and T. Kürner, "The design and applications of high-performance ray-tracing simulation platform for 5G and beyond wireless communications: A tutorial," *IEEE Commun. Surv. Tutorials*, vol. 21, no. 1, pp. 10–27, 2019, doi: 10.1109/COMST.2018.2865724.

[13] N. Al-Falahy, M. Almahamdy, and A. M. Mahmood, "Performance analysis of millimeter wave 5G networks for outdoor environment: Propagation perspectives," *Indones. J. Electr. Eng. Comput. Sci.*, vol. 20, no. 1, pp. 214–221, 2020, doi: 10.11591/ijeecs.v20.i1.pp214-221.

[14] I. Rodriguez *et al.*, "Analysis of 38 GHz mmWave Propagation Characteristics of Urban Scenarios," in *Proceedings of 21st European Wireless Conference, European Wireless 2015*, 2015, pp. 374–381.

[15] F. A. Rodriguez-Corbo, L. Azpilicueta, M. Celaya-Echarri, A. V. Alejos, and F. Falcone, "Propagation Models in Vehicular Communications," *IEEE Access*, vol. 9, no. January, pp. 15902–15913, 2021, doi: 10.1109/ACCESS.2021.3049884.

[16] N. Bias, C. E. O. Lone, H. S. Dhillon, S. Member, and R. M. Buehrer, "Characterizing the First-Arriving Multipath Component in 5G Millimeter Wave Networks :," *IEEE Trans. Wirel. Commun.*, vol. 21, no. 3, pp. 1602–1620, 2022, doi: 10.1109/GLOBECOM38437.2019.9014211.

[17] W. Li, X. Hu, J. Gao, L. Zhao, and T. Jiang, "Measurements and Analysis of Propagation Channels in Vehicle-to-Infrastructure Scenarios," *IEEE Trans. Veh. Technol.*, vol. 69, no. 4, pp. 3550–3561, 2020, doi: 10.1109/TVT.2020.2972150.

[18] F. Alejandro *et al.*, "Deterministic and Empirical Approach for Millimeter-Wave Complex Outdoor Smart Parking Solution Deployments," *Sensors*, vol. 21, no. 4112, pp. 1–16, 2021.

[19] M. B. Majed, T. A. Rahman, O. A. Aziz, and A. Info, "Propagation Path Loss Modeling and Outdoor Coverage Measurements Review in Millimeter Wave Bands for 5G Cellular Communications," *Int. J. Electr. Comput. Eng.*, vol. 8, no. 4, pp. 2254–2260, 2020, doi: 10.11591/ijece.v8i4.pp2254-2260.

[20] D. Cassioli, L. A. Annoni, and S. Piersanti, "Characterization of Path loss and Delay Spread of 60-GHz UWB Channels vs. Frequency," in *IEEE International Conference on Communications*, 2013, no. 6, pp. 5153–5157. doi: 10.1109/ICC.2013.6655401.

[21] J. He and Y. J. Chun, "Performance Analysis for AOA-Based Localization under Millimeter-Wave Wireless Networks," *IEEE Access*, vol. 10, pp. 17221–17230, 2022, doi: 10.1109/ACCESS.2022.3149915.

[22] K. Yu and Y. J. Guo, "Statistical NLOS Identification Based on AOA, TOA, and Signal Strength," *IEEE Trans. Veh. Technol.*, vol. 58, no. 1, pp. 274–286, 2009, doi: 10.1109/TVT.2008.924975.

[23] D. Biswas, S. Barai, and B. Sau, "Improved RSSI Based Vehicle Localization Using Base Station," in *2021 International Conference on Innovative Trends in Information Technology (ICITIIT)*, 2021, pp. 1–6.

[24] J. Li *et al.*, "Directional Analysis of Indoor Massive MIMO Channels at 6 GHz Using SAGE," in *2017 IEEE 85th Vehicular Technology Conference: VTC2017-Spring*, 2017, vol. June, pp. 1–5. doi: 10.1109/VTCSpring.2017.8108203.

[25] C. Mapper, "Instant CAD Files for any Location on Earth," 2020. https://cadmapper.com/ (accessed Mar. 15, 2022).

[26] *Wireless InSite, Reference Manua*, Version 3. Remcom Inc, 2020.

[27] J. Y. Lee, J. H. Lee, and S. C. Kim, "Improving the Accuracy of Millimeter-Wave Ray-Tracing Simulations by Modeling Roadside Trees," *IEEE Antennas Wirel. Propag. Lett.*, vol. 18, no. 1, pp. 162–166, 2019, doi: 10.1109/LAWP.2018.2883633.

[28] A. Klautau, P. Batista, Y. Wang, and R. W. H. Jr, "5G MIMO Data for Machine Learning : Application to Beam-Selection using Deep Learning," 2018. doi: 10.1109/ITA.2018.8503086.

[29] Y. Dong *et al.*, "Channel Characterization for Vehicle-to-Infrastructure Communications in Millimeter-Wave Band," *IEEE Access*, vol. 4, pp. 1–17, 2020, doi: 10.1109/ACCESS.2020.2977208.

[30] D. He, L. Wang, K. Guan, B. Ai, J. Kim, and Z. Zhong, "Channel Characterization for mmWave Vehicle-to-Infrastructure Communications in Urban Street Environment," in *13th European Conference on Antennas and Propagation (EuCAP 2019)*, 2019, no. EuCAP, pp. 1–5.

[31] J. G. Andrews *et al.*, "Modeling and Analyzing Millimeter Wave Cellular Systems," *IEEE Trans. Commun.*, vol. 65, no. 1, pp. 403–430, 2017, doi: 10.1109/TCOMM.2016.2618794.